An Iterative EnKF for Strongly Nonlinear Systems

PAVEL SAKOV

Nansen Environmental and Remote Sensing Center, Bergen, Norway

DEAN S. OLIVER

Uni Centre for Integrated Petroleum Research, Bergen, Norway

LAURENT BERTINO

Nansen Environmental and Remote Sensing Center, Bergen, Norway

(Manuscript received 18 July 2011, in final form 22 November 2011)

ABSTRACT

The study considers an iterative formulation of the ensemble Kalman filter (EnKF) for strongly nonlinear systems in the perfect-model framework. In the first part, a scheme is introduced that is similar to the ensemble randomized maximal likelihood (EnRML) filter by Gu and Oliver. The two new elements in the scheme are the use of the ensemble square root filter instead of the traditional (perturbed observations) EnKF and rescaling of the ensemble anomalies with the ensemble transform matrix from the previous iteration instead of estimating sensitivities between the ensemble observations and ensemble anomalies at the start of the assimilation cycle by linear regression. A simple modification turns the scheme into an ensemble formulation of the iterative extended Kalman filter. The two versions of the algorithm are referred to as the iterative EnKF (IEnKF) and the iterative extended Kalman filter (IEKF).

In the second part, the performance of the IEnKF and IEKF is tested in five numerical experiments: two with the 3-element Lorenz model and three with the 40-element Lorenz model. Both the IEnKF and IEKF show a considerable advantage over the EnKF in strongly nonlinear systems when the quality or density of observations are sufficient to constrain the model to the regime of mainly linear propagation of the ensemble anomalies as well as constraining the fast-growing modes, with a much smaller advantage otherwise.

The IEnKF and IEKF can potentially be used with large-scale models, and can represent a robust and scalable alternative to particle filter (PF) and hybrid PF–EnKF schemes in strongly nonlinear systems.

1. Introduction

a. Motivation

The problem of nonlinearity in ensemble data assimilation has attracted considerable attention in the last few years. Most attempts to use the ensemble framework for nonlinear data assimilation concentrate either on modifying the ensemble Kalman filter (EnKF; Anderson 2010), merging the EnKF and particle filters (Hoteit et al. 2008; Stordal et al. 2011; Lei and Bickel 2011), trying to adapt particle filters to high-dimensional problems (e.g., van Leeuwen 2009), or developing hybrid EnKF-variational data assimilation systems (e.g., Zhang and Zhang 2012). At the same time, research on handling nonlinearity by means of iterations of the EnKF is surprisingly small, limited, to the best of our knowledge, to the ensemble randomized maximal likelihood filter (EnRML; Gu and Oliver 2007) and the running in place scheme (RIP; Kalnay and Yang 2010).

The aim of this study is to consider the use of the EnKF as a linear solution in iterations of the Newton method for minimizing the local (i.e., limited to one assimilation cycle) cost function and investigate the performance of such a scheme in a number of experiments with two common nonlinear chaotic models.

b. Strongly nonlinear systems

Since the introduction of the EnKF by Evensen (1994) it has been often viewed as a robust alternative to the

Corresponding author address: Pavel Sakov, Nansen Environmental and Remote Sensing Center, Thormohlensgate 47, Bergen, 5006 Norway.
E-mail: pavel.sakov@gmail.com

extended Kalman filter (EKF; Smith et al. 1962; Jazwinski 1970), suitable for strongly nonlinear systems. While the robustness of the EnKF is well understood and confirmed by a large body of experimental evidence, the claims about its ability to handle "strongly nonlinear" cases are usually of generic character, without defining what a strongly nonlinear data assimilation (DA) system is. Because the iterative methods studied here are designed primarily for handling strongly nonlinear systems, it is important to define this concept.

The Kalman filter (KF) provides an optimal framework for linear systems, when both the model and observation operator are linear. It yields the optimal solution using sensitivities between perturbations of the model state and observations. It is essential for the KF that these sensitivities remain valid within the characteristic uncertainty intervals (e.g., standard deviations) for the model state and observations encountered by the DA system. In reality the sensitivities in a nonlinear system never stay constant within the characteristic uncertainty intervals; however, in many cases the effects of the nonlinearity are small, and the system can perform nearly optimally using linear solutions. We will refer to such systems as *weakly nonlinear*. And vice versa, the systems with sensitivities that cannot be assumed constant will be referred to as *strongly nonlinear*.

It is important to note that whether a DA system is weakly nonlinear or strongly nonlinear depends not only on the nonlinearity of the model or observations as such, but on the state of the DA system as a whole (Verlaan and Heemink 2001). Depending on the amount and quality of observations, the same nonlinear DA system can be either in a weakly nonlinear or in a strongly nonlinear regime. For example, a system with the 3-element Lorenz model (Lorenz 1963) (referred to hereafter as L3) with observations of each element with observation error variance of 2 taken and assimilated every 5 or even 8 integration steps of 0.01 can be considered as weakly nonlinear; while the same system with observations every 25 steps is essentially a strongly nonlinear system.[1]

The nonlinear behavior of a DA system with chaotic nonlinear model can also be affected by design solutions, such as the length of the DA window. An increase of the DA window leads to the increase of the uncertainty of the model state at the end of the window due to the growing modes. At some point, perturbations with the characteristic magnitude of order of the uncertainty

of the model state can no longer be assumed to propagate mainly linearly about the estimated trajectory, and the system becomes strongly nonlinear. Such (design induced) strongly nonlinear behavior should perhaps be distinguished from the genuine strongly nonlinear situations, such as the above example of the L3-based system with observations every 25 steps.

This study considers the use of the iterative EnKF (IEnKF) for strongly nonlinear systems. Our main interest is the case of a nonlinear system with perfect model and relatively rare but accurate observations, such that the noniterative (linear) solution would not work well (or at all) due to the increase of the forecast error caused by the growing modes.

For the applicability of the KF framework we assume that, while being strongly nonlinear, the system can be constrained to a point when the sensitivities between perturbations of the model state and perturbations of observations can be considered as essentially constant within the characteristic uncertainty intervals (standard deviations) of the model state and observations. If this assumption does not hold, not only more general (nonlinear) minimization methods should be considered for DA; but also the whole estimation framework associated with characterizing uncertainty with second moments and using the least squares cost function becomes questionable.

c. Background

Use of iterative linear methods for nonlinear systems is an established practice in DA. Jazwinski (1970, section 8.3) considers both global (over many assimilation cycles) and local (over a single assimilation cycle) iterations of the EKF. He notes that the use of global iterations loses the recursive nature of the KF, while the use of local iterations retains it. Bell (1994) shows that the global iterative Kalman smoother represents a Gauss–Newton method for maximizing the likelihood function.

This study investigates only local iterations. Concerning global iterations, it is not clear to us how useful they can be for data assimilation with a chaotic nonlinear model if, for example, the noniterative system is prone to divergence.

The iterative methods have already been applied in the EnKF context. The maximum likelihood ensemble filter (MLEF; Zupanski 2005) represents an ensemble based gradient method. It considers iterative minimization of the cost function in ensemble-spanned subspace to handle nonlinear observations (observations with a nonlinear forward operator), but does not consider repropagation of the ensemble. It is therefore aimed at handling strongly nonlinear observations, but

---

[1] In fact, the behavior of the latter system, with observations every 25 steps, can vary between being weakly nonlinear and strongly nonlinear in different assimilation cycles.

not a strongly nonlinear model. Two ensemble-based gradient schemes using an adjoint model are proposed in Li and Reynolds (2009): one with global iterations and its simplified version with local iterations.

Gu and Oliver (2007) introduced a local iterative scheme called EnRML. It is based on the iterative solution for the minimum of the quadratic cost function by the Newton method and by nature is close to the scheme proposed in this paper. The EnRML uses sensitivities calculated by linear regression between the ensemble observations and the initial ensemble anomalies at the beginning of the assimilation cycle. Each iteration of the EnRML involves adjustment of each ensemble member using the traditional (perturbed observations) EnKF (Burgers et al. 1998) and repropagation of the updated ensemble. In the linear case, it is equivalent to the standard (noniterative) EnKF; however, it requires two iterations to detect the linearity. Because the EnRML can handle both nonlinear observations and nonlinear propagation of the ensemble anomalies about the ensemble mean, it can be seen as an extension of the MLEF in this regard. Wang et al. (2010) noticed that the use of the "average" sensitivity matrix in the EnRML is not guaranteed to yield a downhill direction in some cases with very strong nonlinearity, and can lead to divergence. We comment that this situation may be similar to that with the divergence of the Newton (or secant) method; and that the possibility of divergence does not invalidate the method as such, but rather points at its applicability limits.

The scheme proposed in this study is a further development of the EnRML. The most important modification is the use of the ensemble square root filter (ESRF) as a linear solution in the iterative process. Unlike the traditional EnKF, the ESRF uses exact factorization of the estimated state error covariance by the ensemble anomalies and therefore eliminates the suboptimality caused by the stochastic nature of the traditional EnKF. We also use rescaling of the ensemble anomalies before and after propagation instead of regression in the EnRML. The two methods are shown to be mainly equivalent; however, we favor rescaling in this study because it allows a clearer interpretation of the iterative process and seems to have better numerical properties. It also enables turning the IEnKF into the iterative extended Kalman filter (IEKF) by a simple modification.

After formulating the IEnKF, we perform a number of experiments with two simple models. The purpose of these experiments is comparing the performance of the IEnKF against some known benchmarks, setting some new benchmarks, and exploring its capabilities in some rather nontraditional regimes.

The outline of this paper is as follows. The iterative EnKF (IEnKF) scheme is introduced in section 2, its performance is tested in section 3, followed by a discussion and conclusions in sections 4 and 5.

2. IEnKF: The scheme

In the EnKF framework the system state is characterized by the ensemble of model states $\mathbf{E}^{n \times m}$, where n is the state size and m is the ensemble size. The model state estimate $\mathbf{x}$ is carried by the ensemble mean:

$$\mathbf{x} = \frac{1}{m}\mathbf{E1}, \qquad (1)$$

while the model state error covariance estimate $\mathbf{P}$ is carried by the ensemble anomalies:

$$\mathbf{P} = \frac{1}{m-1}\mathbf{AA}^{\mathrm{T}}. \qquad (2)$$

Here $\mathbf{1}$ is a vector with all elements equal to 1 and length matching other terms of the expression, and

$$\mathbf{A} = \mathbf{E} - \mathbf{x1}^{\mathrm{T}}$$

is the matrix of ensemble anomalies and superscript T denotes matrix transposition.

Let us consider a single assimilation cycle from time t_1 to time t_2. To describe iterations within the cycle, we will use subscripts 1 and 2 for variables at times t_1 and t_2, correspondingly, while the superscript will refer to iteration number. Variables without superscripts will denote the final instances obtained in the limit of an infinite number of iterations. In this notation, the initial state of the system in this cycle (that is the analyzed ensemble from the previous cycle) is denoted as $\mathbf{E}_1^0$, while the final state, or the analyzed ensemble, is denoted as $\mathbf{E}_2$. Because only observations from the times $t \leq t_2$ are assimilated to obtain $\mathbf{E}_2$, it represents a filter solution. The $\mathbf{E}_1$ represents the final ensemble at time t_1. Because it is obtained by assimilating observations from $t_2 > t_1$, it is a lag-1 smoother solution. The initial estimate of the system state at the end of this cycle $\mathbf{E}_2^0$ will be referred to as the forecast.

Unlike propagation in weakly nonlinear systems, propagation of the forecast ensemble in a strongly nonlinear system is characterized by divergence of the trajectories due to the presence of unstable modes to such a degree that the sensitivity of observations to the model state becomes substantially different for each ensemble member. Because the system can no longer be characterized by uniform sensitivities, the linear (KF)

solution cannot be used for assimilating observations (at t_2), or becomes strongly suboptimal. The KF solution could work *after* assimilating the observations, as it might reduce the uncertainty (ensemble spread) to a degree when the system could be characterized by uniform sensitivities, but one needs to know these sensitivities *before* the assimilation. The solution is to assimilate using the available, imperfect sensitivities, and then use the improved estimation of the model state error for refining this result. This iterative process is formalized below by means of the Newton method.

Let $\mathcal{M}_{12}$ be the (nonlinear) propagator from time t_1 to t_2, so that

$$\mathbf{x}_2 = \mathcal{M}_{12}(\mathbf{x}_1), \tag{3}$$

where $\mathbf{x}$ is the model state vector. Let $\mathcal{H}_2$ be the (nonlinear) observation operator at time t_2, so that $\mathcal{H}_2(\mathbf{x})$ represents observations at that time associated with the model state $\mathbf{x}$. Let $\mathbf{y}_2$ be observations available at time t_2, with the observation error covariance $\mathbf{R}_2$. Let us seek the solution $\mathbf{x}_1$ as the minimum of the following cost function:

$$\mathbf{x}_1 = \mathrm{argmin}\, \{(\mathbf{x}_1 - \mathbf{x}_1^0)^{\mathrm{T}}(\mathbf{P}_1^0)^{-1}(\mathbf{x}_1 - \mathbf{x}_1^0)$$
$$+ [\mathbf{y}_2 - \mathcal{H}_2(\mathbf{x}_2)]^{\mathrm{T}}(\mathbf{R}_2)^{-1}[\mathbf{y}_2 - \mathcal{H}_2(\mathbf{x}_2)]\}, \tag{4}$$

where $\mathbf{x}_2$ is related with $\mathbf{x}_1$ by (3). Condition of zero gradient of the cost function at its minimum yields

$$(\mathbf{P}_1^0)^{-1}(\mathbf{x}_1 - \mathbf{x}_1^0) - \{\mathbf{\nabla}_{x_1}\mathcal{H}_2[\mathcal{M}_{12}(\mathbf{x}_1)]\}^{\mathrm{T}}(\mathbf{R}_2)^{-1}$$
$$\times \{\mathbf{y}_2 - \mathcal{H}_2[\mathcal{M}_{12}(\mathbf{x}_1)]\} = 0. \tag{5}$$

Let $\mathbf{x}_1^i$ be the approximation for $\mathbf{x}_1$ at ith iteration. Assuming that the propagation and observation operators are smooth enough, and that at some point in the iterative process the difference between system state estimates at successive iterations becomes small, we have

$$\mathcal{M}_{12}(\mathbf{x}_1^{i+1}) = \mathcal{M}_{12}(\mathbf{x}_1^i) + \mathbf{M}_{12}^i(\mathbf{x}_1^{i+1} - \mathbf{x}_1^i)$$
$$+ O(\|\mathbf{x}_1^{i+1} - \mathbf{x}_1^i\|^2), \tag{6}$$

$$\mathbf{\nabla}_{x_1}\mathcal{H}_2[\mathcal{M}_{12}(\mathbf{x}_1^{i+1})] = \mathbf{H}_2^i\mathbf{M}_{12}^i + O(\|\mathbf{x}_1^{i+1} - \mathbf{x}_1^i\|), \tag{7}$$

where

$$\mathbf{M}_{12}^i \equiv \mathbf{\nabla}\mathcal{M}_{12}(\mathbf{x}_1^i),$$

$$\mathbf{H}_2^i \equiv \mathbf{\nabla}\mathcal{H}_2(\mathbf{x}_2^i),$$

and $\|\cdot\|$ denotes a norm. After substituting (6) and (7) into (5) and discarding quadratic terms, we obtain

$$(\mathbf{P}_1^0)^{-1}(\mathbf{x}_1^{i+1} - \mathbf{x}_1^0) + (\mathbf{H}_2^i\mathbf{M}_{12}^i)^{\mathrm{T}}(\mathbf{R}_2)^{-1}\mathbf{H}_2^i\mathbf{M}_{12}^i(\mathbf{x}_1^{i+1} - \mathbf{x}_1^i)$$
$$= (\mathbf{H}_2^i\mathbf{M}_{12}^i)^{\mathrm{T}}(\mathbf{R}_2)^{-1}\{\mathbf{y}_2 - \mathcal{H}_2[\mathcal{M}_{12}(\mathbf{x}_1^i)]\},$$

or, after rearrangement,

$$\mathbf{x}_1^{i+1} = \mathbf{x}_1^i + \mathbf{P}_1^{i+1}(\mathbf{H}_2^i\mathbf{M}_{12}^i)^{\mathrm{T}}(\mathbf{R}_2)^{-1}\{\mathbf{y}_2 - \mathcal{H}_2[\mathcal{M}_{12}(\mathbf{x}_1^i)]\}$$
$$+ \mathbf{P}_1^{i+1}(\mathbf{P}_1^0)^{-1}(\mathbf{x}_1^0 - \mathbf{x}_1^i), \tag{8}$$

where

$$\mathbf{P}_1^{i+1} = [(\mathbf{P}_1^0)^{-1} + (\mathbf{H}_2^i\mathbf{M}_{12}^i)^{\mathrm{T}}(\mathbf{R}_2)^{-1}\mathbf{H}_2^i\mathbf{M}_{12}^i]^{-1}. \tag{9}$$

Substituting

$$(\mathbf{P}_1^0)^{-1} = (\mathbf{P}_1^{i+1})^{-1} - (\mathbf{H}_2^i\mathbf{M}_{12}^i)^{\mathrm{T}}(\mathbf{R}_2)^{-1}\mathbf{H}_2^i\mathbf{M}_{12}^i \tag{10}$$

into the last term of (8), we obtain a slightly different form of the iterative solution:

$$\mathbf{x}_1^{i+1} = \mathbf{x}_1^0 + \mathbf{P}_1^{i+1}(\mathbf{H}_2^i\mathbf{M}_{12}^i)^{\mathrm{T}}(\mathbf{R}_2)^{-1}\{\mathbf{y}_2 - \mathcal{H}_2[\mathcal{M}_{12}(\mathbf{x}_1^i)]$$
$$+ \mathbf{H}_2^i\mathbf{M}_{12}^i(\mathbf{x}_1^i - \mathbf{x}_1^0)\}. \tag{11}$$

Equations (8) and (11) can be written using the Kalman gain (i.e., the sensitivity of the analysis to the innovation):

$$\mathbf{x}_1^{i+1} = \mathbf{x}_1^i + \mathbf{K}_{12}^i\{\mathbf{y}_2 - \mathcal{H}_2[\mathcal{M}_{12}(\mathbf{x}_1^i)]\}$$
$$+ \mathbf{P}_1^{i+1}(\mathbf{P}_1^0)^{-1}(\mathbf{x}_1^0 - \mathbf{x}_1^i) \tag{12}$$

$$= \mathbf{x}_1^0 + \mathbf{K}_{12}^i\{\mathbf{y}_2 - \mathcal{H}_2[\mathcal{M}_{12}(\mathbf{x}_1^i)] + \mathbf{H}_2^i\mathbf{M}_{12}^i(\mathbf{x}_1^i - \mathbf{x}_1^0)\}, \tag{13}$$

where

$$\mathbf{K}_{12}^i = \mathbf{P}_1^{i+1}(\mathbf{H}_2^i\mathbf{M}_{12}^i)^{\mathrm{T}}(\mathbf{R}_2)^{-1}$$
$$= \mathbf{P}_1^0(\mathbf{H}_2^i\mathbf{M}_{12}^i)^{\mathrm{T}}[\mathbf{H}_2^i\mathbf{M}_{12}^i\mathbf{P}_1^0(\mathbf{H}_2^i\mathbf{M}_{12}^i)^{\mathrm{T}} + \mathbf{R}_2]^{-1} \tag{14}$$

is the sensitivity of the analysis at t_1 to the innovation at t_2. Equation (12) is similar to Tarantola [2005, his Eq. (3.51)], while (13) is similar to the basic equation used in the EnRML [Gu and Oliver (2007), see their Eqs. (12) and (13)].

The solutions in (12) or (13) can be used directly in a local iterative EKF for nonlinear perfect-model systems. They are indeed formally equivalent. Equation (12) uses

an increment to the previous iteration, while (13) uses an increment to the initial state. In the linear case

$$\mathcal{H}_2[\mathcal{M}_{12}(\mathbf{x}_1^i)] = \mathcal{H}_2[\mathcal{M}_{12}(\mathbf{x}_1^0)] + \mathbf{H}_2\mathbf{M}_{12}(\mathbf{x}_1^i - \mathbf{x}_1^0),$$

and the final solution is given by the very first iteration in (12) or (13).

We will now adopt (12) to the ensemble formulation, starting from replacing the state error covariance with its factorization in (2) by the ensemble anomalies. The increment yielded by the second terms in the right-hand sides of (12) and (13) can now be represented as a linear combination of the initial ensemble anomalies at t_1:

$$\mathbf{K}_{12}^i\{\mathbf{y}_2 - \mathcal{H}_2[\mathcal{M}_{12}(\mathbf{x}_1^i)]\} = \frac{1}{m-1}\mathbf{A}_1^0(\mathbf{H}_2^i\mathbf{M}_{12}^i\mathbf{A}_1^0)^{\mathrm{T}}$$

$$\times \left[\frac{1}{m-1}\mathbf{H}_2^i\mathbf{M}_{12}^i\mathbf{A}_1^0(\mathbf{H}_2^i\mathbf{M}_{12}^i\mathbf{A}_1^0)^{\mathrm{T}} + \mathbf{R}_2\right]^{-1}$$

$$\times \{\mathbf{y}_2 - \mathcal{H}_2[\mathcal{M}_{12}(\mathbf{x}_1^i)]\} = \mathbf{A}_1^0\mathbf{b}_2^i, \qquad (15)$$

where $\mathbf{b}_2^i$ is a vector of linear coefficients. It can be conveniently expressed via the standardized ensemble observation anomalies[2] $\mathbf{S}_2^i$ and standardized innovation $\mathbf{s}_2^i$ at the ith iteration:

$$\begin{aligned}\mathbf{b}_2^i &= (\mathbf{S}_2^i)^{\mathrm{T}}[\mathbf{I} + \mathbf{S}_2^i(\mathbf{S}_2^i)^{\mathrm{T}}]^{-1}\mathbf{s}_2^i \\ &= [\mathbf{I} + (\mathbf{S}_2^i)^{\mathrm{T}}\mathbf{S}_2^i]^{-1}(\mathbf{S}_2^i)^{\mathrm{T}}\mathbf{s}_2^i,\end{aligned} \qquad (16)$$

where

$$\mathbf{S}_2^i \equiv (\mathbf{R}_2)^{-1/2}\mathbf{H}_2^i\mathbf{M}_{12}^i\mathbf{A}_1^0/\sqrt{m-1}, \qquad (17)$$

$$\mathbf{s}_2^i \equiv (\mathbf{R}_2)^{-1/2}[\mathbf{y}_2 - \mathcal{H}_2(\mathbf{x}_2^i)]/\sqrt{m-1}. \qquad (18)$$

The product $\mathbf{H}_2^i\mathbf{M}_{12}^i\mathbf{A}_1^0$ in (17) can be interpreted as the initial ensemble anomalies propagated with the current estimate $\mathbf{M}_{12}^i$ of the tangent linear propagator and observed with the current estimate $\mathbf{H}_2^i$ of the gradient (Jacobian) of the observation operator.

The EnKF does not require explicit estimation of the tangent linear propagator; it is implicitly carried by the "cloud" of ensemble anomalies. Because the ensemble anomalies in the EnKF do factorize the state error covariance, their magnitude depends on the estimated state error. Hence, the approximation of the tangent linear propagator in the EnKF depends on the estimated state error; unlike that in the EKF, where a point estimation of the tangent linear propagator is used. This

also applies to the gradient of the observation operator. As a result, the system's nonlinearity in the EnKF not only manifests itself through the nonlinear propagation and nonlinear observation of the state estimate, but also contributes to the estimates of the state error and to implicit estimates of the gradients of the propagation and observation operators contained in the clouds of ensemble anomalies and ensemble observation anomalies. This entanglement of the estimated state error covariance and nonlinearity may be one of the main reasons for the observed robustness of the EnKF.

In line with this reasoning, for consistent estimates of the gradients of the propagation and observation operators we need to set the ensemble anomalies at t_1 in accordance with the current estimate of the state error covariance.

In the Kalman filter the analyzed state error covariance can be calculated through a refactorization of the cost function so that it absorbs the contribution from the assimilated observations (see e.g., Hunt et al. 2007, their section 2.1). It is technically difficult to obtain a formal estimate for the state error covariance in the iterative process; however, the estimate in (9) is consistent with the linear solution used in iterations, and it yields the correct solution at the end of the iterative process if the uncertainty in the system state reduces to such degree that propagation of the ensemble anomalies from time t_1 to t_2 becomes essentially linear. For these reasons, we adopt (9) as the current estimate for the state error covariance in the iterative process. After that, we can exploit its similarity with the Kalman filter solution and use the ensemble transform matrix (ETM) calculated at time t_2 to update the ensemble anomalies at time t_1:

$$\mathbf{A}_1^i = \mathbf{A}_1^0\mathbf{T}_2^i, \qquad (19)$$

where the particular expression for the ETM $\mathbf{T}_2^i$ depends on the chosen EnKF scheme.

Applying the ETM calculated at one time to the ensemble at a different time makes no difference to the system in the linear case and will therefore result in the correct solution if propagation of the ensemble anomalies becomes essentially linear at the end of the iterative process. The same applies to the nonlinearity of the observation operator. Note, however, that in the case of synchronous data assimilation (when the assimilation is conducted at the time of observations) with a nonlinear observation operator, there is no need to repropagate the ensemble if the propagation operator is linear.

As will be discussed later, DA in a strongly nonlinear system requires a rather high degree of optimality. This suggests using an update scheme with exact factorization of the analyzed state error covariance (i.e., the ESRF).

---

[2] "Ensemble observation anomalies" refer to forecast ensemble perturbations in the observation space.

In particular, one can use the ETKF (Bishop et al. 2001) as the most common choice:

$$\mathbf{T}_2^i = [\mathbf{I} + (\mathbf{S}_2^{i-1})^{\mathrm{T}}\mathbf{S}_2^{i-1}]^{-1/2}. \qquad (20)$$

To finalize calculation of $\mathbf{b}_2^i$ and $\mathbf{T}_2^i$ we now need to estimate the product $\mathbf{H}_2^i\mathbf{M}_{12}^i\mathbf{A}_1^0$ in (17). Because the gradients are applied not to the current ensemble anomalies $\mathbf{A}_1^i$ but to the initial ensemble anomalies[3] $\mathbf{A}_1^0$, to obtain the approximation for $\mathbf{H}_2^i\mathbf{M}_{12}^i\mathbf{A}_1^0$ we need to rescale $\mathbf{H}_2^i\mathbf{M}_{12}^i\mathbf{A}_1^i$ by using the transform inverse to (19):

$$\mathbf{H}_2^i\mathbf{M}_{12}^i\mathbf{A}_1^0 \leftarrow \mathcal{H}_2[\mathcal{M}_{12}(\mathbf{E}_1^i)]\left(\mathbf{I} - \frac{1}{m}\mathbf{1}\mathbf{1}^{\mathrm{T}}\right)(\mathbf{T}_2^i)^{-1}, \qquad (21)$$

where $\mathbf{E}_1^i$ is the ensemble at the ith iteration at time t_1: $\mathbf{E}_1^i = \mathbf{x}_1^i\mathbf{1}^{\mathrm{T}} + \mathbf{A}_1^i$. In this way, the magnitudes of the ensemble anomalies during nonlinear propagation and observation are consistent with the assumed current estimate of the state error covariance, while the ensemble anomalies used in the assimilation are consistent with the initial state error covariance. In the linear case the consecutive application of $\mathbf{T}_2^i$ and $(\mathbf{T}_2^i)^{-1}$ results in an identity operation.

Another possible approach (Gu and Oliver 2007) is to use linear regression between the observation ensemble anomalies at t_2 and ensemble anomalies at t_1 for estimating the product $\mathbf{H}_2^i\mathbf{M}_{12}^i$:

$$\mathbf{H}_2^i\mathbf{M}_{12}^i \approx \mathcal{H}_2[\mathcal{M}_{12}(\mathbf{E}_1^i)]\left(\mathbf{I} - \frac{1}{m}\mathbf{1}\mathbf{1}^{\mathrm{T}}\right)(\mathbf{A}_1^i)^{\dagger}, \qquad (22)$$

where "$\dagger$" denotes pseudo inverse. If $m \leq n$, then the approaches (21) and (22) are formally equivalent (see appendix A):

$$\left(\mathbf{I} - \frac{1}{m}\mathbf{1}\mathbf{1}^{\mathrm{T}}\right)(\mathbf{A}_1^i)^{\dagger}\mathbf{A}_1^0 = \left(\mathbf{I} - \frac{1}{m}\mathbf{1}\mathbf{1}^{\mathrm{T}}\right)(\mathbf{T}_2^i)^{-1}.$$

In a nonlinear system with $m > n$ the rescaling and regression are no longer equivalent. Numerical experiments indicate that they yield approximately equal RMSE, but may differ in regard to the system's stability (not shown).

Finally, let us consider the third term in (12). Using factorizations for $\mathbf{P}_1^i$ and $\mathbf{P}_1^0$ along with (19), we obtain:

$$\begin{aligned}\mathbf{P}_1^{i+1}(\mathbf{P}_1^0)^{-1} &= \mathbf{A}_1^{i+1}(\mathbf{A}_1^{i+1})^{\mathrm{T}}[\mathbf{A}_1^0(\mathbf{A}_1^0)^{\mathrm{T}}]^{\dagger} \\ &= \mathbf{A}_1^0\mathbf{T}_2^{i+1}(\mathbf{T}_2^{i+1})^{\mathrm{T}}(\mathbf{A}_1^0)^{\mathrm{T}}[\mathbf{A}_1^0(\mathbf{A}_1^0)^{\mathrm{T}}]^{\dagger} \\ &= \mathbf{A}_1^0\mathbf{T}_2^{i+1}(\mathbf{T}_2^{i+1})^{\mathrm{T}}[(\mathbf{A}_1^0)^{\mathrm{T}}\mathbf{A}_1^0]^{\dagger}(\mathbf{A}_1^0)^{\mathrm{T}}. \end{aligned} \qquad (23)$$

---

[3] In this way the scheme avoids multiple assimilation of the same observations.

In this form calculating $\mathbf{P}_1^{i+1}(\mathbf{P}_1^0)^{-1}$ involves a pseudoinversion of only an $m \times m$ matrix.

The rescaling procedure described above can be modified by scaling with a factor ϵ instead of the ETM $\mathbf{T}_2^i$:

$$\mathbf{A}_1^i = \epsilon\mathbf{A}_1^0,$$

where $\epsilon = \mathrm{const} \ll 1$. The ensemble anomalies are scaled back after propagation, before analysis:

$$\mathbf{A}_2^i \leftarrow \mathbf{A}_2^i/\epsilon,$$

so that instead of (21) we have

$$\mathbf{H}_2^i\mathbf{M}_{12}^i\mathbf{A}_1^0 \approx \mathcal{H}_2[\mathcal{M}_{12}(\mathbf{x}_1^i\mathbf{1}^{\mathrm{T}} + \epsilon\mathbf{A}_1^0)]\left(\mathbf{I} - \frac{1}{m}\mathbf{1}\mathbf{1}^{\mathrm{T}}\right)\frac{1}{\epsilon}. \qquad (24)$$

In this way, and the scheme calculates a numerical estimation of the product $\mathbf{H}_2^i\mathbf{M}_{12}^i$ at a point rather than its approximation with an ensemble of finite spread. The final (analyzed) ensemble anomalies are calculated at the very last iteration by applying the ETM to the propagated ensemble anomalies. This modification turns the scheme into a state space representation of the iterative EKF that, similar to the EnKF, requires no explicit calculation of the gradients of the propagation and observation operators. Note that normally this scheme is not sensitive to the magnitude of ϵ, which is similar to the insensitivity to the magnitude of displacement vector in numerical differentiation.

To distinguish the variants of the scheme described above, we will refer to the first one (with the rescaling by the ETM) as the iterative EnKF, or IEnKF, and to the second one (with rescaling by a small factor) as the iterative EKF, or IEKF. The pseudocode for the IEnKF and EKF is presented in appendix B.

The formulation of the IEnKF with the rescaling by the ETM proposed above has some similarity with the RIP scheme (Kalnay and Yang 2010). Both schemes apply the ensemble update transforms calculated at time t_2 for updating the ensemble at time t_1. However, there is a substantial difference between the IEnKF and RIP. RIP applies updates in an incremental way (i.e., the next update is applied to the previous update) until it achieves the *best fit to observations*. This is equivalent to discarding the background term in the cost function and looking for a solution of the optimization problem in the ensemble range. This approach can make sense for a strongly nonlinear system when the background term becomes negligible compared to the observation term due to the strong growth of ensemble anomalies between observations, but it loses consistency in estimation of the state error covariance and may be prone to overfitting.

Despite these doubts, the RIP is reported to obtain good performance in tests and realistic applications. A scheme similar to the RIP based on the traditional EnKF is proposed in Lorentzen and Nævdal (2011).

3. Experiments

This section investigates the performance of the IEnKF and IEKF in a number of experiments with small models. We conduct five experiments, starting with two experiments with the 3-element Lorenz model (Lorenz 1963), followed by three experiments with the 40-element Lorenz model (Lorenz and Emanuel 1998). In the first two experiments we compare the performance of the IEnKF and IEKF with that of the other schemes reported in the literature, in the third experiment we set up a case with conditions favorable for the application of the IEnKF, and the last two experiments are designed to expose the limits of the applicability of the IEnKF in the perfect model framework. All experiments involve no localization.

Three schemes are compared in each test: IEnKF, IEKF, and EnKF.[4] In all experiments the iterations are stopped as soon as the root-mean-square of the increment to the previous iteration given by the second and third terms in the right-hand side of (8) becomes smaller than $10^{-3}\sigma_{obs}$, where σ_{obs}^2 is the observation error variance used in the experiment. The maximal number of iterations in all experiments is set to 20. In experiments with the IEKF the value $\epsilon = 10^{-4}$ is used for the rescaling multiple. Observations are noncorrelated and have equal error variance. The magnitude of inflation in runs with L3 and L40 models is tuned to the best performance from a set of values with the step of 0.02 when not exceeding 1.10 (0.98, 1.00, 1.02, ..., 1.10), and with the step of 0.05 when exceeding 1.10 (1.10, 1.15, ...); unless otherwise stated. Inflation is applied to the analyzed ensemble anomalies.[5] The RMSE is calculated at each assimilation cycle as a square root of the mean quadratic error of all elements of the model state:

$$\text{RMSE}(\mathbf{x}, \mathbf{x}^{\text{true}}) = \left[\frac{1}{n}(\mathbf{x} - \mathbf{x}^{\text{true}})^{\text{T}}(\mathbf{x} - \mathbf{x}^{\text{true}})\right]^{1/2},$$

where $\mathbf{x}$ and $\mathbf{x}^{\text{true}}$ are the estimated and true model states, respectively; and n is the length of the model state vector. The RMSE value averaged over specified number of cycles is used to characterize the performance of a scheme for a given configuration. The initial ensemble, true field, and observations used in a given experiment for different schemes are identical.

The Matlab code for the experiments is available online (http://enkf.nersc.no/Code/IEnKF_paper_Matlab_code). The core code is close to the pseudocode in appendix B, with one additional feature: we limit the minimal singular value of the ETM calculated at line 30 of the pseudocode by a small number of about 3×10^{-3}; this prevents instability that can develop in some cases with stronger nonlinearity and larger ensembles (e.g., in experiment 3 with $m = 60$ and no rotations).

a. Experiments with the 3-element Lorenz model

In this section we run experiments with two configurations of the 3-element Lorenz model (L3; Lorenz 1963). Both configurations have been used in previous studies.

For the model we use a finite-difference approximation of the following system of ordinary differential equations:

$$\dot{x} = \sigma(y - x),$$

$$\dot{y} = \rho x - y - xz,$$

$$\dot{z} = xy - \beta z,$$

where $\sigma = 10$, $\rho = 28$, and $\beta = 8/3$. This system is integrated with the fourth-order Runge–Kutta scheme, using a fixed time step of 0.01; one integration step is considered to be a model step. Note that the settings of the integrator are essential parameters of the numerical model that affect the model's dynamic behavior.

The ensemble is initialized by a set of randomly chosen states from a large collection of states from a long run of the model.

1) EXPERIMENT 1

The settings of this experiment were initially used in Miller et al. (1994), and after that in a number of studies on data assimilation (Evensen 1997; Yang et al. 2006; Kalnay et al. 2007). It therefore represents not just one of many possible designs, but one of the established test beds for data assimilation with nonlinear systems. The small size of the state (just three elements) reduces the computational expense and makes it possible to concentrate on schemes rather than implementation details. Further, there is an extensive literature on the dynamic properties of the 3-element Lorenz model (e.g., Trevisan and Pancotti 1998), which is very helpful for understanding and interpreting the behavior of the system.

Three observations are made every $T = 25$ model steps, which is one of each model state element. The

---

[4] We use the term EnKF in a generic sense here. Specifically, we use an ESRF solution.

[5] For bigger magnitudes of inflation applying it to the ensemble anomalies *before* assimilation can in some instances improve the performance of the system, while degrading it in other instances.

observation errors are Gaussian with zero mean and error variance: $\sigma^2_{obs} = 2$. The system is run for 51 000 assimilation cycles, and the first 1000 cycles are discarded. The results averaged over 50 000 cycles are presented in Table 1.

We observe that the IEnKF and the IEKF show the best overall performance. For comparison, for the same setup, Kalnay et al. (2007) reported the RMSE of 0.71 for the EnKF, $m = 3$; 0.59 for the EnKF, $m = 6$; 0.53 for 4D-Var with the optimal assimilation window of 75 time steps; and Yang et al. (2006) reported the RMSE of 0.63 for the EKF. The RIP scheme achieves the RMSE of 0.35 with $m = 3$, inflation of 1.047, and random perturbations of magnitude of 7×10^{-4} (Yang et al. 2012).

Increasing the ensemble size from $m = 3$ to $m = 10$ yields a substantial improvement for the EnKF, some improvement for the IEnKF, and no improvement for the IEKF. Furthermore, it is known that ESRF systems with large ensembles are prone to gradual buildup of non-Gaussian ensemble distributions (Lawson and Hansen 2004) that can be "corrected" by applying mean preserving ensemble rotations (Sakov and Oke 2008). For this reason, when the ensemble size exceeds the state size, we repeat experiments twice by running them with and without random mean-preserving ensemble rotations after each analysis. In this experiment the rotations improve the performance of the EnKF, but not IEnKF or IEKF.

This indifference of the performance of the IEKF to the ensemble rotations is also observed in other experiments presented below. We therefore do not report these results.

The average number of iterations for the IEnKF and IEKF is quite low, below 3. This is explained by the

TABLE 1. Performance statistics for experiment 1: L3 model, $T = 25$, $p = 3$, and $\sigma^2_{obs} = 2$. The numbers in parentheses refer to runs with mean preserving random ensemble rotations applied after each analysis.

Estimate	Scheme		
	EnKF	IEnKF	IEKF
$m = 3$			
Analysis rmse	0.82	0.33	0.32
No. of iterations	1	2.8	2.7
Inflation used	1.35	1.08	1.06
$m = 10$			
Analysis rmse	0.65 (0.59)	0.30 (0.31)	0.32
No. of iterations	1	2.6 (2.6)	2.7
Inflation used	1.15 (1.04)	1.02 (1.00)	1.06

character of this system, which is weakly nonlinear most of the time, and only becomes strongly nonlinear during transitions from one quasi-stable state to another. Figure 1 shows the RMSE for every iteration during a randomly chosen sequence of 100 assimilation cycles. The maximal number of iterations required for convergence in each cycle is 4. The RMSE for the iteration before last is not shown, as it is undistinguishable from the RMSE for the last iteration. It can be seen that there is little change in the RMSE after the second iteration. In some instances, DA increases the RMSE, which is not unexpected, due to the presence of observation error. Yet, there are a few instances (e.g., cycle 81) when there is a considerable improvement in the RMSE at the third and further iterations. These are the instances when the system undergoes transition between quasi-stable states and exhibits a strongly nonlinear behavior.
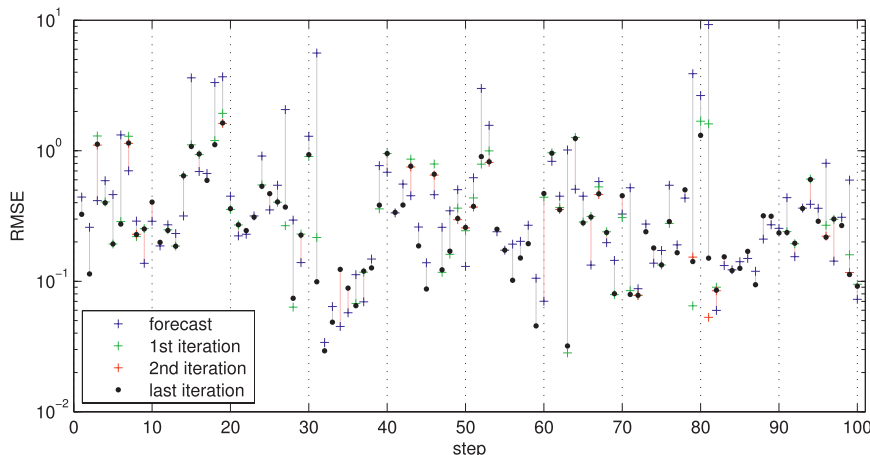

FIG. 1. The RMSE of the IEnKF in experiment 1 at each iteration for randomly chosen 100 assimilation cycles. The vertical lines show the difference between the forecast RMSE and the analysis RMSE; the gray lines correspond to the instances when the RMSE has reduced and the pink lines correspond to when the RMSE has increased.

2) EXPERIMENT 2

The settings of this experiment were used in Anderson (2010). The system is run with observations of each state vector element made every 12 steps with error variance equal to 8. It is run for 101 000 assimilation cycles, and the first 1000 cycles are discarded. The results averaged over 100 000 cycles are presented in Table 2. The RMSE for the IEnKF and IEKF is considerably better than that for the EnKF. Comparing the IEnKF and IEKF, the IEnKF shows lower RMSE, achieved with fewer iterations and smaller inflation, and therefore seems to represent a more robust option for this setup than the IEKF. Anderson (2010, his Fig. 10) reported RMSE exceeding 1.10 for this setup for the EAKF, traditional EnKF, and the rank histogram filter (RHF).

The random mean-preserving ensemble rotations improve performance of both the EnKF and IEnKF.

b. Experiments with the 40-element Lorenz model

In this section we conduct experiments with three configurations of the 40-element Lorenz model (L40; Lorenz and Emanuel 1998). The model is based on the 40 coupled ordinary differential equations in a periodic domain:

$$\dot{x}_i = (x_{i+1} - x_{i-2})x_{i-1} - x_i + 8, \quad i = 1, \ldots, 40;$$
$$x_0 = x_{40}, \quad x_{-1} = x_{39}, \quad x_{41} = x_1.$$

Following Lorenz and Emanuel (1998), this system is integrated with the fourth-order Runge–Kutta scheme, using a fixed time step of 0.05, which is considered to be one model step.

The experiments with L40 are run with ensemble sizes of $m = 25$ and 60. The ensemble size of 25 is the size when an EnKF–L40 system with standard settings[6] without localization is expected to show some small, but statistically significant deterioration in performance compared to that with larger ensembles (e.g., Sakov and Oke 2008; Anderson 2010). The idea behind using a smaller ensemble than necessary for the best performance is to mimic some common conditions for large-scale EnKF applications. The ensemble size of 60 is chosen to test whether the systems can benefit from a larger ensemble.

1) EXPERIMENT 3

This setup is based on "standard" settings used in a number of studies, but with a much longer interval between observations. The intention is to make the

TABLE 2. Performance statistics for experiment 2: L3 model, $T = 12$, $p = 3$, and $\sigma_{obs}^2 = 8$. The numbers in parentheses refer to runs with ensemble rotations.

Estimate	Scheme		
	EnKF	IEnKF	IEKF
$m = 3$			
Analysis rmse	1.00	0.64	0.69
No. of iterations	1	2.7	2.8
Inflation used	1.08	1.06	1.08
$m = 10$			
Analysis rmse	0.91 (0.86)	0.60 (0.57)	0.69
No. of iterations	1	2.6 (2.5)	2.8
Inflation used	1.04 (1.04)	1.02 (1.00)	1.08

system more nonlinear, so that propagation of the ensemble anomalies starts exhibiting a substantial nonlinearity toward the end of the assimilation cycle. At the same time, we try to design a test that would be suitable for using the Newton method, which is a test where the system changes from being strongly nonlinear to weakly nonlinear during iterations.

Each element of the state is observed with error variance of $\sigma_{obs}^2 = 1$ every $T = 12$ steps. Both the ensemble and true field are randomly initialized from a set of 200 model states that represent an established ensemble obtained at the end of a long run of the system with the standard settings (observations made every model step) and ensemble size of 200. The system is integrated for 51 000 assimilation cycles; the first 1000 cycles are excluded from the statistics.

The results of this experiment are summarized in Table 3. The average number of iterations for both iterative schemes is quite high: 9.1 for the IEnKF and 10.0 for the IEKF. This indicates that, unlike L3 systems in experiments 1 and 2, this L40 system remains in the strongly nonlinear state at all times, rather than during occasional transitions. For all schemes the forecast spread is greater than 1, which points at a substantial nonlinearity during the initial propagation of the ensemble anomalies for this model; however, the analysis RMSE of 0.48 for the IEnKF points at a rather weak nonlinearity at the end of the iterative process, so that this experiment can be considered as suitable for application of the Newton method.[7]

Concerning individual performances of each scheme, the IEnKF is the best performer, both by direct metric (RMSE) and indirect indicators, such as the inflation, number of iterations, and consistency between the RMSE and the ensemble spread. Despite the relatively

---

[6] By "standard settings" we mean 40 observations, one per state vector element, made every time step, with an observation error variance of 1.

[7] Ideally, we would like to further reduce the analysis RMSE while keeping the forecast RMSE >1 to make the transition between the linear and nonlinear regimes more evident, but we could not achieve stable runs in these conditions.

TABLE 3. Performance statistics for experiment 3: L40 model, $T = 12$, $p = 40$, and $\sigma^2_{\text{obs}} = 1$. The numbers in parentheses refer to runs with ensemble rotations.

Estimate	Scheme		
	EnKF	IEnKF	IEKF
$m = 25$			
Analysis rmse	1.47	0.48	0.60
Analysis spread	1.15	0.51	0.69
Forecast spread	2.26	1.28	1.98
No. of iterations	1	9.1	10.0
Inflation used	1.80	1.20	1.50
$m = 60$			
Analysis rmse	0.78 (0.76)	0.46 (0.44)	0.59
Analysis spread	0.84 (0.80)	0.50 (0.46)	0.70
Forecast spread	1.88 (1.87)	1.25 (1.19)	2.00
No. of iterations	1	9.7 (7.9)	9.9
Inflation used	1.25 (1.20)	1.15 (1.10)	1.50

high value of the inflation (1.20) at which it reaches the best RMSE, the scheme also behaves robustly for much smaller inflation magnitudes, with the RMSE of 0.59 at $1 + \delta = 1.08$ and 0.64 at 1.06.

The IEKF is the second best performer with the RMSE of 0.60, but it needs a rather high inflation of 1.50 to achieve it. Investigating the exact mechanism behind such behavior of the IEKF (why does it need that high

inflation) is beyond the scope of this paper. We suggest that it may be related to the lower robustness of the point estimation of sensitivities in the IEKF (i.e., 24) versus the finite spread approximation in the IEnKF (i.e., 21) in conditions when the cost function may develop multiple minima, which is a known phenomenon in nonlinear systems with long assimilation windows (e.g., Miller et al. 1994, see their Fig. 6).

Repeating the experiment with a larger ensemble size shows that the EnKF would have substantially benefited from it, as it reaches the RMSE of 0.78 with the ensemble size of $m = 60$ and inflation of $1 + \delta = 1.25$. Both the IEnKF and IEKF show only a rather minor benefit from this increase in the ensemble size. The ensemble rotations once again yield small but statistically significant reduction of the RMSE for the EnKF and IEnKF, but not for the IEKF.

Figure 2 shows analysis RMSE of the EnKF, IEnKF, and EKF depending on the interval between observations T. As expected, there is little difference between these schemes in weakly nonlinear regimes. Interestingly, the EnKF outperforms the IEKF for the intervals between observations $T = 1$ and $T = 2$. For $T \geq 4$ the iterative schemes start to outperform the EnKF. With a further increase of nonlinearity the performance
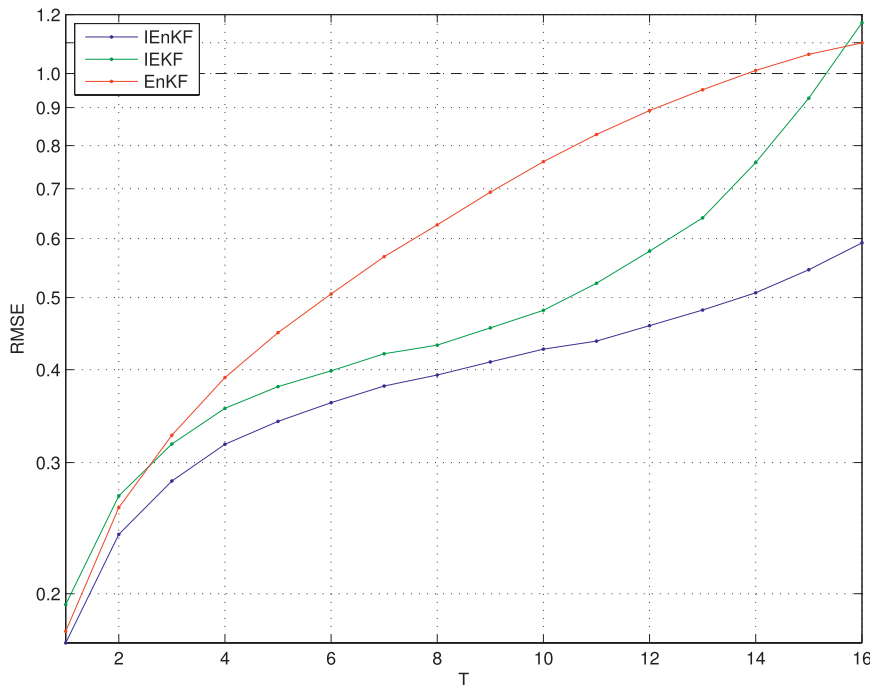

FIG. 2. RMSE of the IEnKF, IEKF, and EnKF with L40 model, depending on the interval between observations T. Observations of every state vector element with observation error variance of 1 are made every T steps. The ensemble size is 40. The inflation is chosen to minimize the RMSE. The dashed horizontal line shows the RMSE of the system with direct insertion of observations.

of the IEKF starts to deteriorate and at some point matches that of the EnKF, although this happens when the RMSE is already greater than the standard deviation of the observation error.

2) EXPERIMENT 4

In the second setup with the L40 model the assimilation is complicated by observing only each fifth or fourth element of the state vector. The intention is to investigate the benefits of using iterative schemes in conditions of sparse observations.

Generally, we find that decreasing space resolution causes greater problems for systems with the L40 model than decreasing time resolution. For example, we could not reliably run any of the tested systems when observing every eighth element every 8 model steps, regardless of the magnitude of observation error variance, while the IEnKF can run stably with observing every fifth element every 12 steps when observation error is very small. From the testing point of view, the main difficulty with configurations considered in this section is that a scheme may seem to perform perfectly well, only to break up at an assimilation cycle number well into thousands, which indicates instability.

In this test the observation error variance is set to $\sigma_{obs}^2 = 10^{-3}$, and once again the ensemble size is $m = 25$. Because the ensemble spreads in this test are much smaller than in the previous test, to avoid divergence during the initial transient period, we initialize the ensemble and the true field from an established system run with 40 observations made at each model step, with observation error variance of 0.1 (cf. 1 in the previous section). To reduce the influence of the system instability, we use shorter runs: the system is integrated for 12 625 assimilation cycles, and the first 125 cycles are excluded from the statistics. Furthermore, we conduct the runs with 4 different initial seeds, and consider a scheme successful for a given configuration if it completes 3 runs out of 4. We then combine statistics from the successful runs.

Table 4 presents the results of experiments with observations of every fifth element ($p = 8$); and then with observations of every fourth element ($p = 10$). RMSE indicates that all systems run in a weakly nonlinear regime only; however, we were not able to achieve consistent performance with a considerably higher observation error variance, which would make the tested systems more nonlinear.

These results show that the tested schemes are differentiated in this experiment by stability rather than by RMSE. When the length of the assimilation window reduces below some critical value (with the number of observations being fixed), all schemes start to run stably and on almost equal footing.

TABLE 4. Performance statistics for experiment 4: L40 model, $\sigma_{obs}^2 = 10^{-3}$, and $m = 25$.

Estimate	Scheme		
	EnKF	IEnKF	IEKF
$p = 8, T = 7$			
Analysis rmse	0.036	0.031	0.033
No. of iterations	1	3.2	3.2
Inflation used	1.06	1.02	1.10
$p = 8, T = 6$			
Analysis rmse	0.031	0.028	0.029
No. of iterations	1	3.1	3.1
Inflation used	1.04	1.02	1.06
$p = 10, T = 12$			
Analysis rmse	—	0.034	—
No. of iterations	—	3.7	—
Inflation used	—	1.06	—
$p = 10, T = 10$			
Analysis rmse	—	0.030	0.032
No. of iterations	—	3.3	3.3
Inflation used	—	1.02	1.15
$p = 10, T = 8$			
Analysis rmse	0.032	0.027	0.028
No. of iterations	1	3.1	3.1
Inflation used	1.10	1.02	1.08

This behavior of the tested DA systems is somewhat different from that described in the previous section. To understand the reasons behind it, we compare the magnitudes of growth of perturbations with the largest singular value of the inverse ETM. Figures 3 and 4 show behavior of two metrics, $\|\mathbf{T}^{-1}\|$ and $\|\mathbf{A}_2^0\|/\|\mathbf{A}_1^0\|$, using the largest singular value as a norm, for an arbitrary chosen interval of 200 assimilation cycles, for the IEnKF, for experiments 3 and 4.

It follows from Fig. 3 that for experiment 3 the magnitude of growth of the ensemble anomalies during the cycle is largely matched by the largest singular value of the inverse ETM or, equivalently, by the reduction of the largest singular value of the ensemble observation anomalies $\mathbf{HA}$ in the update (because for noncorrelated observations with equal error variance, $\mathbf{R} = r\mathbf{I}$, $r = $ const, we have $\|\mathbf{T}^{-1}\| = \|\mathbf{HA}_2^0\|/\|\mathbf{HA}_2^0\mathbf{T}\| = \|\mathbf{HA}_2^0\|/\|\mathbf{HA}_2\|$). For a linear system and uniform diagonal observation error covariance ($\mathbf{R} = \sigma_{obs}^2\mathbf{I}$) there would be a complete match between the two norms, but with nonlinear propagation, there is some observed mismatch in the figure indeed, which can be expected to be rather small. In fact, the run average of the ratio $\mu = \|\mathbf{T}^{-1}\|\|\mathbf{A}_1^0\|/\|\mathbf{A}_2^0\|$ remarkably (within 0.1%) matches the inflation magnitude used in all runs in experiment 3.

By contrast, as follows from Fig. 4, the two metrics do no longer match for experiment 4. We observe that the maximal shrink of the ensemble anomalies in any given direction during the update is, generally, much greater than the perturbation growth during the propagation.
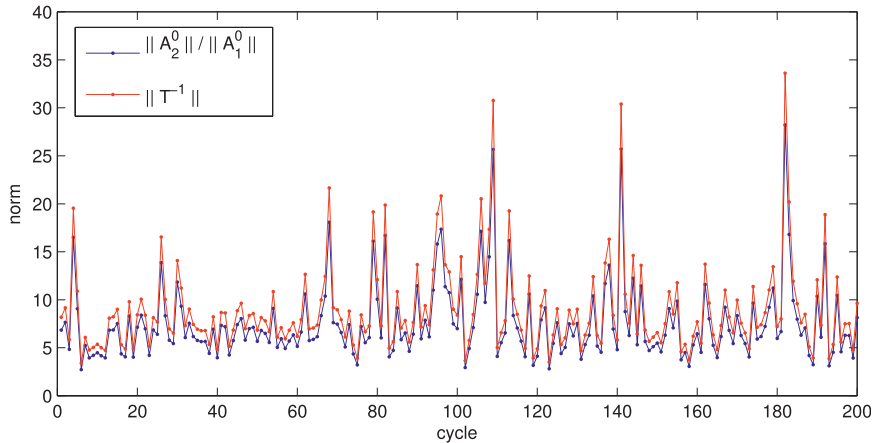
FIG. 3. Behavior of metrics $\|\mathbf{A}_2^0\|/\|\mathbf{A}_1^0\|$ and $\|\mathbf{T}^{-1}\|$ for the IEnKF with L40, $T = 12$, $p = 40$, $\sigma_{\text{obs}}^2 = 1$, and $m = 25$. The biggest singular value is used for the matrix norm.

More specifically, for the IEnKF run with $p = 10$ and $T = 10$ we have $\overline{\mu} = 2.24$, while $1 + \delta = 1.02$; and for the IEKF run with the same parameters $\overline{\mu} = 3.44$, while $1 + \delta = 1.20$. Because for an established system the perturbation growth must, on average, be balanced by the reduction of the ensemble spread during the update, this mismatch means that, generally, in this regime the direction of the largest reduction of the spread of ensemble anomalies during the update does not necessarily coincide with the direction of the largest growth of the ensemble anomalies. Obviously, with fewer observations in experiment 4 than in experiment 3, the variability of the ensemble observation anomalies is no longer representative of that of the ensemble anomalies. In other words, the number of observations is too small for the DA to work out the main variability modes of the system and reliably constrain the growing modes.

Overall, the IEnKF yields the best stability in experiments in this section, followed by the IEKF, and then by the EnKF. The exact mechanism of improving stability by iterative schemes is not clear, but their demonstrated advantage is rather insignificant; moreover, with a larger ensemble the EnKF quickly closes the gap in stability (not shown).[8]

3) EXPERIMENT 5

In the last series of experiments we test each scheme in conditions of dense and frequent but inaccurate observations, so that the ensemble anomalies propagate nonlinearly, but the growth of the anomalies during the assimilation cycle is relatively small because of its short

length. Nonlinear propagation of the ensemble anomalies invalidates the use of the linear solution, either in iterative or noniterative frameworks, so that both EnKF and IEnKF frameworks become strongly suboptimal.

Specifically, we use the L40 model and 40 observations (one per each model state element) with error variance of 20 made at each model step. This configuration is run with ensembles of 25 and 60 members. Because of the much shorter interval between observations than in the previous experiments, the inflation is tuned with the precision of 0.01 (1, 1.01, 1.02, . . . , etc.). The system is run for 101 000 cycles, and the first 1000 cycles are discarded. The results averaged over 100 000 cycles are presented in Table 5. It can be seen that the RMSE (and ensemble spread, not shown) exceeds 1, which signifies for L40 model a strongly nonlinear regime. Unlike experiments 1, 2, and 3, the initial spread does not substantially reduce during iterations, and is unable to reach to the point when propagation of ensemble anomalies about the ensemble mean becomes essentially linear. This makes all involved schemes suboptimal. It follows from the results that, despite the strongly nonlinear regime, there is no major difference between various schemes in these conditions. Moreover, increasing the ensemble size of the EnKF to $m = 60$ reduces the RMSE to 1.08, overperforming the more computationally expensive IEnKF with $m = 25$, as the latter requires on average 3.1 iterations per cycle. The IEKF has the highest RMSE, by some margin, and perhaps should be avoided in these conditions.

4. Discussion

All experiments show good performance of the IEnKF and IEKF schemes in strongly nonlinear systems (except

---

[8] With 60 members and random rotations the EnKF can complete the test for $p = 8$, $T = 8$ with the RMSE of 0.44 at $1 + \delta = 1.08$.
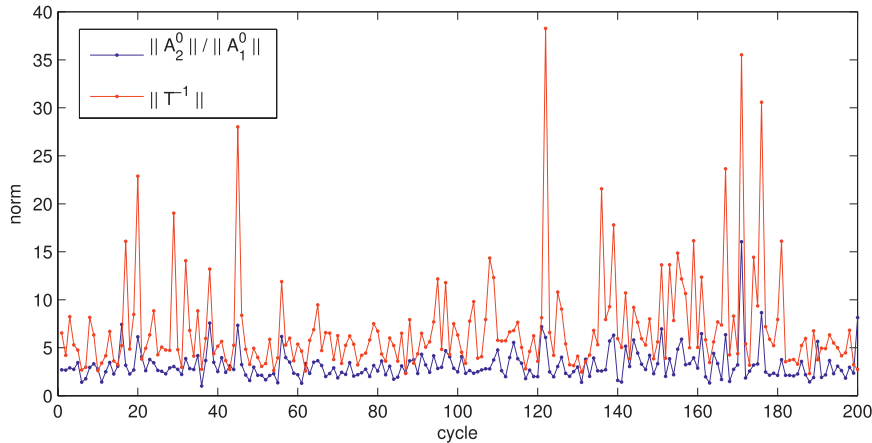
FIG. 4. As in Fig. 3, but for $T = 10$, $p = 10$, $\sigma_{obs}^2 = 10^{-3}$, and $m = 25$.

experiment 5 where the EnKF outperformed the IEKF). Both methods use ensemble estimations of the sensitivity of the modeled observations at t_2 to the initial ensemble anomalies at t_1 (given by the product $\mathbf{M}_{12}^i\mathbf{H}_2^i$); however, there is a substantial conceptual difference between them. The IEnKF approximates sensitivities using an ensemble with spread that characterizes the estimated state error, and (with one possible exception) it showed overall better and more robust performance in the experiments. The IEKF calculates sensitivities by numerical differentiation, using an ensemble with an effectively infinitesimally small spread. Unlike the IEnKF, changes in the system state between iterations for the IEKF involve only recentering of the ensemble, but do not affect the perturbation structure; the latter is only modified at the end of the cycle by means of the ETM and inflation (lines 25 and 26 of the pseudocode in appendix B) to maintain a consistent estimate of the state error.

Comparing the performance of the IEnKF and IEKF with that of the EnKF, we observe that although the iterative schemes work remarkably well in many strongly nonlinear settings, the EnKF is still able to constrain the model in most cases. Its performance can be characterized as overall rather robust, so that taking into account its much lower computational cost, the EnKF should still be considered in practice as the first choice candidate. Furthermore, the fact that the EnKF is able to constrain strongly nonlinear systems in the experiments leaves open the possibility of using global iterative schemes in strongly nonlinear systems with chaotic nonlinear models. Potentially, a global iterative scheme may obtain better results, because with a nonlinear system it is no longer possible to split the global optimization problem into a series of local problems, like in the KF.

The experiments show that strongly nonlinear systems based on the EnKF and (to a lesser degree) IEnKF can often benefit from increased ensemble size. When run with larger ensembles, these systems also, generally, benefit from applying random mean preserving ensemble rotations. (In one instance, in experiment 3, the rotations are even necessary for stability of the IEnKF.) The rotations prevent the buildup of non-Gaussianity in the ensemble that is often associated with larger ensemble sizes in nonlinear ESRF-based systems (Lawson and Hansen 2004; Sakov and Oke 2008; Anderson 2010). The fact that systems with the IEKF do not improve performance with either larger ensembles or/and ensemble rotations suggests that the observed improvements are associated with the finite ensemble spread in the EnKF and IEnKF. This possibly excludes the analytical properties of the ensemble transform in the ESRF as the underlying reason for the development of non-Gaussianity.

We now discuss some general issues related to the use of the iterative schemes.

a. Strong nonlinearity and optimality

The strong nonlinearity in a system can be caused by nonlinear model and/or nonlinear observations, and can

TABLE 5. Performance statistics for experiment 5: L40 model, $T = 1$, $p = 20$, and $\sigma_{obs}^2 = 20$. The numbers in parentheses refer to runs with ensemble rotations.

	Scheme		
Estimate	EnKF	IEnKF	IEKF
$m = 25$			
Analysis rmse	1.27	1.15	1.55
No. of iterations	1	3.1	3.8
Inflation used	1.04	1.04	1.10
$m = 60$			
Analysis rmse	1.08 (1.03)	1.03 (1.00)	1.48
No. of iterations	1	3.1 (3.0)	3.8
Inflation used	1.02 (1.03)	1.02 (1.02)	1.10

manifest itself in a number of different regimes. In the experiments conducted in this study we concentrated on the model nonlinearity. We showed that there are at least three qualitatively different regimes possible. The first regime is characterized by relatively rare but accurate observations, so that the model is generally well constrained, but propagation of the ensemble anomalies is initially (at first iteration) nonlinear as a result of the growth of perturbations. It becomes mainly/more linear in the iterative process due to the reduction of the uncertainty in the system state. The second regime is the regime with very accurate but infrequent and sparse observations. The model is well constrained most of the time, but the system is prone to instability. The third regime is that with relatively frequent but inaccurate observations, so that the system is generally not constrained to the level necessary for linear propagation of the anomalies at any point of the iterative process.

It follows from the experiments that systems running in the first regime can benefit most from using iterative schemes. However, this regime also implies strong corrections, as they must balance the error growth due to growing modes. A strong correction, in turn, implies a (nearly) optimal system, because in the KF the covariance update is obtained from the second-order terms balance (Hunt et al. 2007, their section 2.1). It is only possible to obtain a good second-order balance if there is a nearly perfect first-order balance during the correction of the mean. This means that a strongly nonlinear DA must have a high degree of optimality: a nearly perfect model, sufficiently large ensemble, and sufficient observations. This requirement of optimality may be the biggest practical obstacle to DA in real-world applications with strongly nonlinear systems, such as biogeochemical or land systems, if indeed these systems do run in the first of the three regimes identified above.

Furthermore, we can foresee a situation when the system can potentially be constrained to a weakly nonlinear regime, but the initial estimation of sensitivities is grossly wrong, so that iterations based on the linear solution cannot converge to the correct minimum of the cost function. This can happen, for example, in some cycles in experiment 1 if the interval between observations is increased from 25 to 60 model steps (not shown). In such situations, the system could benefit from using more general minimization methods.

As a somewhat different perspective of the optimality issue, the results of experiments with the L40 model in experiments 4 and 5 show that in suboptimal conditions the more advanced schemes do not necessarily have a big advantage over simpler schemes, and using the EnKF may be the best practical option.

Another aspect of the system is related to the optimality of the linear scheme used in iterations. We have run a number of comparisons between using the ESRF and the traditional EnKF (TEnKF), and overall could see a clear advantage of using the ESRF. For example, in experiment 1 using the TEnKF with the ensemble size $m = 3$ is indeed completely nonfeasible. Equally, in experiment 3 the IEnKF with the TEnKF could not get on par with the IEnKF–ESRF, achieving only RMSE of 1.09 with the inflation 1.50 and using all allowed 20 iterations at each cycle. Increasing the size of the ensemble makes it possible for the IEnKF–TEnKF to reach almost or complete parity with the IEnKF–ESRF in terms of the RMSE, but not necessarily in terms of the number of iterations. With the ensemble size of $m = 10$ in experiment 1 the IEnKF–TEnKF has the RMSE of 0.34 with the inflation 1.04; in experiment 3 with the ensemble size of $m = 60$ and inflation of 1.25 it reaches the RMSE of 0.47, but requires 17.3 iterations on cycle on average versus 9.1 for the IEnKF–ESRF.

b. Localization

To be applicable for large-scale applications, a state space scheme must use localization to avoid rank deficiency. However, localization induces suboptimality, and it remains unclear at the moment how compatible localization is with the requirement of optimality in systems with substantial nonlinear growth.

c. Relative computational effectiveness of different schemes

All iterative schemes in this study require at least two iterations at each assimilation cycle. In weakly nonlinear systems the benefits of increasing the ensemble rank by a factor of 2 can be expected to outweigh those from using an iterative scheme; therefore, it should be normally preferable to use the EnKF in these cases. The same applies to suboptimal situations, when the benefits from using iterative schemes may be rather limited.

It is possible however that in some situations, like in experiment 1, when the system is only weakly nonlinear most of the time, there may be a way to detect the instances of strong nonlinearity by analyzing the innovation, and only use iterative schemes in these instances. However, this approach requires a high degree of confidence in the model, and in practice a larger innovation magnitude may often be caused rather by a model or observation error than by a state transition.

d. Asynchronous observations

In practice it may be difficult or impossible to synchronize the end of each data assimilation cycle with the time of all assimilated observations. It is therefore

important for a scheme to be able to assimilate observations asynchronously. It is known now that the EnKF can be easily adopted to assimilate asynchronous observations by simply using in the analysis the ensemble observations $\mathcal{H}(\mathbf{E})$ estimated at the time of each observation (Hunt et al. 2007), provided that propagation of the ensemble anomalies about the truth is mainly linear (Sakov et al. 2010). This assumption may not hold in some systems, for example in systems that do not constrain the model enough for the linear propagation of anomalies, like in experiment 5. However, if the anomalies do propagate mainly linearly during the *last* iteration of the IEnKF, there are no technical obstacles to using asynchronous observations in the IEnKF in the same way as in the EnKF.

e. Inflation

The proposed schemes generally require use of inflation for better stability and performance. The use of inflation can be seen either as a common practical solution or as an intrinsic deficiency of a scheme caused by the neglect of undersampling. There are a number of studies aimed at developing inflation-less schemes. Houtekamer and Mitchell for a number of years propose the use of multiensemble EnKF configurations for cross validation, and have recently reported a near-operational implementation with no need for inflation (Houtekamer and Mitchell 2009). Bocquet (2011) introduced a new class of EnKF-like schemes derived from a new prior (background) probability density function conditional on the forecast ensemble.

5. Conclusions

This study considers an iterative formulation of the EnKF, referred to as IEnKF. The IEnKF represents a consistent iterative scheme that uses the Newton method for minimizing the cost function at each assimilation cycle, using the EnKF as the linear solution. It inherits from the EnKF its main advantages and therefore can be potentially suitable for use with large-scale models. The IEnKF is equivalent to the EnKF for linear systems, except for additional computations related to the second iteration of the assimilation cycle that is necessary for detecting the linearity. A simple modification of the IEnKF makes it equivalent to the iterative EKF.

Both the IEnKF and IEKF show good results in tests with simple perfect models, with the IEnKF showing overall better performance, both in terms of RMSE and consistency (lower inflation and a better match between the RMSE and the ensemble spread). While the IEnKF always outperforms the EnKF in the conducted experiments, the experiments also indicate that the iterative

schemes may be most beneficial in situations with relatively rare but accurate observations, when it is possible to constrain the system from strongly nonlinear to weakly nonlinear state in the iterative process and, although not shown here, the IEnKF is equally applicable to situations in which not just the system, but the observation operator is nonlinear. Also, while the IEnKF can be implemented as either an iterative form of the ESRF or the traditional EnKF, we observed strong advantages to the ESRF form of the filter, with smaller RMSE when the ensemble size is small, and fewer iterations when the ensemble size is large. The iterative schemes are shown to be less beneficial in suboptimal situations, when the quality or density of observations are insufficient to constrain the model to the regime of mainly linear propagation of the ensemble anomalies or to constrain the fast-growing modes.

APPENDIX A

Proposition

Let $\mathbf{A}$ be an $n \times m$ matrix such that $\mathbf{A1} = 0$, $\mathrm{rank}(\mathbf{A}) = m - 1$, and let $\mathbf{T}$ be an invertible symmetric $m \times m$ matrix such that $\mathbf{T1} = \mathbf{1}$. Then

$$\left(\mathbf{I} - \frac{1}{m}\mathbf{11}^{\mathrm{T}}\right)(\mathbf{AT})^{\dagger}\mathbf{A} = \left(\mathbf{I} - \frac{1}{m}\mathbf{11}^{\mathrm{T}}\right)\mathbf{T}^{-1}. \quad (\mathrm{A1})$$

The proof is outlined below.

1) If $\mathrm{rank}(\mathbf{A}) = m - 1$, then $1/\sqrt{m}$ is the only right singular vector of $\mathbf{A}$ with zero singular value, and

$$\mathbf{A}^{\dagger}\mathbf{A} = \mathbf{I} - \frac{1}{m}\mathbf{11}^{\mathrm{T}}. \quad (\mathrm{A2})$$

2) We now show that $(\mathbf{AT})^{\dagger} = \mathbf{T}^{-1}\mathbf{A}^{\dagger}$. Let us introduce $\mathbf{B} = \mathbf{AT}$ and $\mathbf{C} = \mathbf{T}^{-1}\mathbf{A}^{\dagger}$. By definition, $\mathbf{C}$ is a pseudoinverse of $\mathbf{B}$ if $\mathbf{BCB} = \mathbf{B}$, $\mathbf{CBC} = \mathbf{C}$, $\mathbf{BC}$ is Hermitian, and $\mathbf{CB}$ is Hermitian. Only the last condition is nontrivial, but is satisfied because of (A2):

$$\mathbf{CB} = \mathbf{T}^{-1}\mathbf{A}^{\dagger}\mathbf{AT} = \mathbf{T}^{-1}\left(\mathbf{I} - \frac{1}{m}\mathbf{11}^{\mathrm{T}}\right)\mathbf{T} = \mathbf{I} - \frac{1}{m}\mathbf{11}^{\mathrm{T}}.$$

3) Finally,

$$\left(\mathbf{I} - \frac{1}{m}\mathbf{1}\mathbf{1}^{\mathrm{T}}\right)\mathbf{T}^{-1}\mathbf{A}^{\dagger}\mathbf{A}$$

$$= \left(\mathbf{I} - \frac{1}{m}\mathbf{1}\mathbf{1}^{\mathrm{T}}\right)\mathbf{T}^{-1}\left(\mathbf{I} - \frac{1}{m}\mathbf{1}\mathbf{1}^{\mathrm{T}}\right)$$

$$= \left(\mathbf{I} - \frac{1}{m}\mathbf{1}\mathbf{1}^{\mathrm{T}}\right)\mathbf{T}^{-1}.$$

APPENDIX B

Pseudocode for the IEnKF and IEKF

Presented below is the pseudocode for one assimilation cycle of the IEnKF and IEKF. This pseudocode is rather simplistic and written for maximal clarity. It underlies the similarity of the IEnKF and IEKF and is not optimized specifically for any one of them. It is also not optimized for performance, apart from conducting expensive matrix operations (inversions and powers) in ensemble space. Here ϵ denotes a small parameter used for rescaling in the IEKF, ϵ_0 is another small parameter used for stopping the iterations, and δ is the inflation magnitude that needs to be tuned for each particular configuration of the system. The lines starting with "IEnKF: " or "IEKF: " are specific to the IEnKF or IEKF only:

```
01 function[E₂ᵃ] = ienkf_cycle(E₁⁰, y₂, R₂, M₁₂, H₂)
02    x₁⁰ = E₁⁰1/m
03    A₁⁰ = E₁⁰ − x₁⁰1ᵀ
04    x₁ = x₁⁰
05    IEnKF:   T = I
06    loop
07       IEnKF:   A₁ = A₁⁰T
08       IEKF:    A₁ = εA₁⁰
09       E₁ = x₁1ᵀ + A₁
10       E₂ = M₁₂(E₁)
11       (HE)₂ = H₂(E₂)
12       (Hx)₂ = (HE)₂1/m
13       (HA)₂ = (HE)₂ − (Hx)₂1ᵀ
14       IEnKF:   (HA)₂ = (HA)₂T⁻¹
15       IEKF:    (HA)₂ = (HA)₂/ε
16       (δy)₂ = y₂ − (Hx)₂
17       s = R₂⁻¹ᐟ²(δy)₂/√(m−1)
18       S = R₂⁻¹ᐟ²(HA)₂/√(m−1)
19       G = (I + SᵀS)⁻¹
20       b = GSᵀs
21       (δx)₁ = A₁⁰b + A₁⁰G[(A₁⁰)ᵀA₁⁰]†(A₁⁰)ᵀ(x₁⁰ − x₁)
22       if ‖(δx)₁‖ <= ε₀
23          x₂ = E₂1/m
24          A₂ = (E₂ − x₂1ᵀ)
25          IEKF:   A₂ = A₂G¹ᐟ²/ε
```

```
26          E₂ᵃ = x₂1ᵀ + A₂(1 + δ)
27       return
28       end if
29       x₁ = x₁ + (δx)₁
30       IEnKF:   T = G¹ᐟ²
31    end loop
32 end function.
```

REFERENCES

Anderson, J. L., 2010: A non-Gaussian ensemble filter update for data assimilation. *Mon. Wea. Rev.,* **138,** 4186–4198.

Bell, B. M., 1994: The iterated Kalman smoother as a Gauss–Newton method. *SIAM J. Optim.,* **4,** 626–636.

Bishop, C. H., B. Etherton, and S. J. Majumdar, 2001: Adaptive sampling with the ensemble transform Kalman filter. Part I: Theoretical aspects. *Mon. Wea. Rev.,* **129,** 420–436.

Bocquet, M., 2011: Ensemble Kalman filtering without the intrinsic need for inflation. *Nonlinear Processes Geophys.,* **18,** 735–750.

Burgers, G., P. J. van Leeuwen, and G. Evensen, 1998: Analysis scheme in the ensemble Kalman filter. *Mon. Wea. Rev.,* **126,** 1719–1724.

Evensen, G., 1994: Sequential data assimilation with a nonlinear quasi-geostrophic model using Monte-Carlo methods to forecast error statistics. *J. Geophys. Res.,* **99,** 10 143–10 162.

——, 1997: Advanced data assimilation for strongly nonlinear dynamics. *Mon. Wea. Rev.,* **125,** 1342–1354.

Gu, Y., and D. S. Oliver, 2007: An iterative ensemble Kalman filter for multiphase fluid flow data assimilation. *SPE J.,* **12,** 438–446.

Hoteit, I., D.-T. Pham, G. Triantafyllou, and G. Korres, 2008: A new approximate solution of the optimal nonlinear filter for data assimilation in meteorology and oceanography. *Mon. Wea. Rev.,* **136,** 317–334.

Houtekamer, P. L., and H. L. Mitchell, 2009: Model error representation in an operational ensemble Kalman filter. *Mon. Wea. Rev.,* **137,** 2126–2142.

Hunt, B. R., E. J. Kostelich, and I. Szunyogh, 2007: Efficient data assimilation for spatiotemporal chaos: A local ensemble transform Kalman filter. *Physica D,* **230,** 112–126.

Jazwinski, A. H., 1970: *Stochastic Processes and Filtering Theory.* Academic Press, 376 pp.

Kalnay, E., and S.-C. Yang, 2010: Accelerating the spin-up of Ensemble Kalman Filtering. *Quart. J. Roy. Meteor. Soc.,* **136,** 1644–1651.

——, H. Li, T. Miyoshi, S.-C. Yang, and J. Ballabrera-Poy, 2007: 4-D-Var or ensemble Kalman filter? *Tellus,* **59A,** 758–773.

Lawson, W. G., and J. A. Hansen, 2004: Implications of stochastic and deterministic filters as ensemble-based data assimilation methods in varying regimes of error growth. *Mon. Wea. Rev.,* **132,** 1966–1981.

Lei, J., and P. Bickel, 2011: A moment matching ensemble filter for nonlinear non-Gaussian data assimilation. *Mon. Wea. Rev.,* **139,** 3964–3973.

Li, G., and A. Reynolds, 2009: Iterative ensemble Kalman filters for data assimilation. *SPE J.,* **14,** 496–505.

Lorentzen, R. J., and G. Nævdal, 2011: An iterative ensemble Kalman filter. *IEEE Trans. Automat. Contrib.,* **56** (8), 1990–1995.

Lorenz, E. N., 1963: Deterministic nonperiodic flow. *J. Atmos. Sci.,* **20,** 130–141.

——, and K. A. Emanuel, 1998: Optimal sites for suplementary weather observations: Simulation with a small model. *J. Atmos. Sci.,* **55,** 399–414.

Miller, R. N., M. Ghil, and F. Gauthiez, 1994: Advanced data assimilation in strongly nonlinear dynamical systems. *J. Atmos. Sci.,* **51,** 1037–1056.

Sakov, P., and P. R. Oke, 2008: Implications of the form of the ensemble transformations in the ensemble square root filters. *Mon. Wea. Rev.,* **136,** 1042–1053.

——, G. Evensen, and L. Bertino, 2010: Asynchronous data assimilation with the EnKF. *Tellus,* **62A,** 24–29.

Smith, G. L., S. F. Schmidt, and L. A. McGee, 1962: Application of statistical filtering to the optimal estimation of position and velocity on-board a circumlunar vehicle. NASA Tech. Rep. R-135, 27 pp.

Stordal, A., H. Karlsen, G. Nævdal, H. Skaug, and B. Vallés, 2011: Bridging the ensemble Kalman filter and particle filters: The adaptive Gaussian mixture filter. *Comput. Geosci.,* **15,** 293–305.

Tarantola, A., 2005: *Inverse Problem Theory and Methods for Parameter Estimation.* SIAM, 342 pp.

Trevisan, A., and F. Pancotti, 1998: Periodic orbits, Lyapunov vectors, and singular vectors in the Lorenz system. *J. Atmos. Sci.,* **55,** 390–398.

van Leeuwen, P. J., 2009: Particle filtering in geophysical systems. *Mon. Wea. Rev.,* **137,** 4089–4114.

Verlaan, M., and A. W. Heemink, 2001: Nonlinearity in data assimilation applications: A practical method for analysis. *Mon. Wea. Rev.,* **129,** 1578–1589.

Wang, Y., G. Li, and A. C. Reynolds, 2010: Estimation of depths of fluid contacts by history matching using iterative ensemble Kalman smoothers. *SPE J.,* **15,** 509–525.

Yang, S.-C., E. Kalnay, and B. Hunt, 2012: Handling nonlinearity in an ensemble Kalman filter: Experiments with the three-variable Lorenz model. *Mon. Wea. Rev.,* in press.

——, and Coauthors, 2006: Data assimilation as synchronization of truth and model: Experiments with the three-variable Lorenz system. *J. Atmos. Sci.,* **63,** 2340–2354.

Zhang, M., and F. Zhang, 2012: E4DVar: Coupling an ensemble Kalman filter with four-dimensional variational data assimilation in a limited-area weather prediction model. *Mon. Wea. Rev.,* **140,** 587–600.

Zupanski, M., 2005: Maximum likelihood ensemble filter: Theoretical aspects. *Mon. Wea. Rev.,* **133,** 1710–1726.